molecular pharmaceutics

Article

pubs.acs.org/molecularpharmaceutics

A Unique Bicellar Nanosystem Combining Two Effects on Stratum Corneum Lipids

Gelen Rodríguez,*[,†] Mercedes Cócera,[†] Laia Rubio,[†] Carmen López-Iglesias,[‡] Ramon Pons,[†] Alfons de la Maza,[†] and Olga López[†]

[†]Department of Chemical and Surfactants Technology, Institute of Advanced Chemistry of Catalonia (IQAC-CSIC), C/ Jordi Girona 18-26, 08034 Barcelona, Spain

[‡]University of Barcelona's Scientific and Technological Centers (CCiT-UB), Barcelona Science Park, C/ Baldiri Reixac, 10, 08028 Barcelona, Spain

ABSTRACT: In this work a new composition (dioleylphosphatidylcholine, DOPC, and dihexanoylphosphocholine, DHPC) is used to form the bicellar system and to evaluate their effect on stratum corneum (SC) lipids. Through this article, "bicellar system" will refer to a lipid binary system in which lipids are self-assembled forming different nanostructures. DOPC/DHPC system is characterized by dynamic light scattering and cryo-transmission electron microscopy showing two different nanostructures: unilamellar vesicles and tubular structures. In order to study the SC lipid organization attenuated total reflectance Fourier transform infrared spectroscopy, freeze-substitution applied to transmission electron microscopy and X-ray scattering are used. This work compares for the first time the use of two different X-ray scattering methods, transmission with synchrotron radiation and grazing incidence with conventional source, for skin studies. Our results indicate that vesicle-shaped structures remain adhered to the SC surface being unable to penetrate into the skin probably due to their large and voluminous size, while a proportion of structures could have interaction with SC lipids increasing the lamellar organization. Thus, the different nanostructures present in the system have different effects on SC lipids. The appropriate combination of both effects and the possibility to incorporate drugs offer a range of possibilities for the DOPC/DHPC system in development for skin care products.

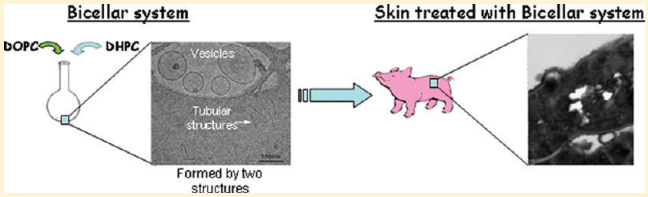

KEYWORDS: *bicellar system, lipid organization, stratum corneum, unsaturated phospholipid, X-ray scattering, delivery system*

INTRODUCTION

The study of skin is a very important topic in the pharmaceutical field because of its role as an alternative route to systemic administration. Recent developments in transdermal drug delivery systems are focused on methods showing systemic and topical efficacy. The skin barrier function is mainly due to the specific composition and organization of stratum corneum (SC) lipids.[1−3] The SC is the outermost part of the epidermis and consists of a very thin layer of flat anucleated cells (the corneocytes) surrounded by a lipid matrix organized in a lamellar structure (the intercellular lipids), which are a mixture composed mainly of ceramides, cholesterol and fatty acids.[4−6]

Our group is studying the effect of new systems composed of phospholipids (bicelles) on the skin, specifically over molecular organization of the SC lipids.[7−9] The word "bicelle"[10] refers to a discoidal micelle formed by a bilayer of dimyristoylphosphocholine (DMPC) closed in the edges by dihexanoylphosphocholine (DHPC). These systems have been used for skin purposes because bicelles avoid the use of potentially irritant surfactants, and have properties such as modulable structure, and small enough size for skin penetration that could be useful in dermatological, cosmetic, and/or pharmaceutical applications. Depending on the temperature, the molar ratio between long- and short-chain phospholipids, and/or the total lipid concentration, these structures may form a progression of nanostructures from small discoidal micelles to cylindrical micelles, perforated lamellar sheets or vesicles.[11,12] Due to this morphological versatility a consensus about a unique word to define all of these nanostructures does not exist. Pabst et al.[13] proposed "bicelle lipid mixture" and Triba et al.[14] referred to "binary lipid mixtures" to name these complex systems. Throughout this article, we will call them "bicellar system".

Recently, we reported that changes in the composition and/or gel-to-liquid crystalline phase transition temperature (T_m) of long-chain phospholipids that build bicelles induce specific effects of these nanostructures on the skin barrier function. Mainly two kinds of bicelles have been studied, one formed by dipalmitoylphosphocoline (DPPC) and DHPC and another formed by DMPC/DHPC.[8,15,16] In both cases, the long-chain phospholipid is formed by saturated fatty acids. Yokomizo et al. reported that phospholipids containing unsaturated fatty acids in the hydrophobic group, as DOPC, are strong penetration enhancers for percutaneous delivery of some topically applied

Received: February 16, 2011
Revised: January 11, 2012
Accepted: January 20, 2012
Published: January 20, 2012

drugs.[17] Moreover, Pereira-Lachataignerais et al. demonstrated that a mixture of DOPC and the surfactant sodium dodecyl sulfate (SDS) exhibited similar morphological versatility to the bicellar system.[18]

The present work proposes the use of DOPC as long-chain phospholipid and DHPC, instead of the surfactant SDS proposed by Pereira-Lachataignerais et al., as short-chain phospholipid that is milder than SDS for skin purposes. The objective of this work is to use a new composition to form a bicellar system and to evaluate their effect on SC lipids.

Some of the more useful techniques for studies of SC lipid organization are attenuated total reflectance Fourier transform infrared (ATR-FTIR) spectroscopy, X-ray scattering and microscopy. The vibrational characteristic frequencies of the alkyl chain lipids related to differently ordered phases have been extensively reported by ATR-FTIR.[8,19,20] Alkyl chain arrangement of the SC lamellar structure exhibits higher order in the gel phase (orthorhombic and hexagonal) than in the liquid-crystalline phase. The X-ray scattering techniques also provide information about the molecular organization of lipids.[18] Small-angle X-ray scattering (SAXS) is used to obtain information about the repeat distance of the lipid lamellar phase. The present work compares for the first time two different methods about this technique for skin studies: transmission incidence with synchrotron radiation and grazing incidence with conventional X-ray source (GISAXS). Both methods provide the same type of information, but GISAXS is more sensitive to the surface[21] and it is an ideal tool to characterize the structures in three dimensions.[22] In recent works, our group reported on the use of this configuration for skin studies.[8,9] On the other hand, SAXS has been extensively used to study the lamellar lipid structure of the SC with the incident beam parallel and perpendicular to the SC plane.[23,24]

In addition, freeze-substitution transmission electron microscopy (FSTEM) gives great evidence of the localization of different structures in SC and of the SC lipid lamellar structure after treatment with this system.[4,25]

All in all, the present work introduces a new lipid nanostructured system formed by DOPC/DHPC able to modify the SC lipid lamellae. This new system and its effect on lipid organization of the SC have been evaluated by means of the aforementioned techniques, and the relevant data obtained should be considered in future development of skin care products.

EXPERIMENTAL SECTION

Chemicals. The lipids 1,2-dioleyl-*sn*-glycero-3-phosphatidylcholine (DOPC), and 1,2-dihexanoyl-*sn*-glycero-3-phosphatidylcholine (DHPC), purity greater than 99%, were purchased from Avanti Polar Lipids (Alabaster, Al). Purified water was obtained by an ultrapure water system, Milli-Q plus 185 (Millipore, Bedford, MA). For washing purposes sodium lauryl ether sulfate (SLES) solution at 0.5% w/v from Sigma-Aldrich Chemie GmbH (Steinheim, Germany) was used. To isolate the SC from the full skin, trypsin (from porcine pancreas) from Sigma-Aldrich Chemie GmbH (Steinheim, Germany) and phosphate buffered saline tablets from Sigma Chemical CO. (St. Louis, MO) were used.

Preparation and Characterization of the Bicellar System. Samples were prepared by mixing appropriate amounts of DOPC and DHPC in chloroform solutions to reach DOPC/DHPC molar ratio 3.5. After mixing the components, the chloroform was removed with a rotary evaporator and the sample was kept under 1 atm vacuum for 2 h. After that, the systems were hydrated with Milli-Q water to reach 20% (w/v) of total lipid concentration. The system was prepared by subjecting the sample to several cycles of sonication/freezing. Several cycles of five minutes of sonication in a bath sonicator Ultrasons-H (P-Selecta, Barcelona, Spain) at 40 °C and subsequent freezing at −80 °C (below the T_m of the DOPC, which is −20 °C[26]) were performed until the sample became a stable milky dispersion at room temperature. The system was characterized by dynamic light scattering (DLS) and cryo-transmission electron microscopy (cryo-TEM) techniques and maintained under refrigeration (≈4 °C) until use.

For control purposes the system was centrifuged twice, for 20 min at 20000*g*, every time, in an Eppendorf centrifuge 5415 (Hamburg, Germany). The supernatant and the precipitate were examined by DLS.

Dynamic Light Scattering (DLS). The hydrodynamic diameter (HD) and polydispersity index were determined by means of DLS using a Zetasizer Nano ZS (Malvern Systems, Southborough, MA) that provides the size distribution curves. The DLS measures the self-diffusion coefficient of the particles due to Brownian motion. The relationship between the size of a particle and its self-diffusion coefficient is defined by the Stokes−Einstein equation:

$$\mathrm{HD} = kT/3\pi\eta D$$

where HD is the hydrodynamic diameter, D is the translational diffusion coefficient, k is the Boltzmann's constant, T is the absolute temperature and η is the viscosity.

The instrument uses a 632 nm wavelength laser beam. The noninvasive backscattering technology was used in order to minimize multiple scattering effects without the need of diluting the samples. The detection of the light scattered was performed at an angle of 173°. The measurement was performed at room temperature. The signal treatment was elaborated using the software provided by Malvern Instruments.

Cryo-Transmission Electron Microscopy (Cryo-TEM). The morphology of the bicellar system was evaluated by cryo-TEM. A thin aqueous film was formed by dipping and withdrawing a bare specimen grid from the suspension. Glow-discharged holey carbon grids were used. After withdrawal from suspension the grid was blotted against filter paper, leaving thin sample films spanning the grid holes. These films were vitrified by plunging the grid into ethane, which was kept at its melting point by liquid nitrogen,[27] using a Vitrobot (FEI Company, Eindhoven, Netherlands) and keeping the sample before freezing at 100% humidity. The temperature at which the thin films were kept, where vitrification was initiated, was room temperature. The vitreous sample films were transferred to a microscope Tecnai F20 (FEI Company, Eindhoven, Netherlands) using a Gatan cryotransfer (Barcelona, Spain). The visualization was taken at 200 kV at a temperature between −170 °C and −175 °C using low-dose imaging conditions.

Skin Preparation. Porcine skin was selected considering two facts: this skin has been reported as the most suitable model of those available in the absence of human tissue,[28] and the present work is based on the study of the microstructural modifications visualized by transmission electron microscopy. Using this technique, microstructure of SC from both species is almost indistinguishable.[29]

For ATR-FTIR Experiments. Porcine skin was obtained from the back of experimental animals in the Department of Dermatology, University Hospital Clinic of Barcelona (Spain), 2−3 h after the animals were sacrificed. The bristles were

removed carefully with an animal clipper, and then the skin was washed with tap water. The excised skin was dermatomed to 500 ± 50 μm thickness (dermatome GA630, Aesculap, Tuttlingen, Germany). Then, full skin containing dermis, epidermis and SC was used to perform the experiments.

Isolation of the SC for X-ray Scattering Experiments and FSTEM Experiments. Sections of fresh pig skin were heated with the SC side in contact with a metal plate for 10 s at 80 °C, and the epidermis was scraped off in sheets.[30] To isolate the SC the epidermal sheets were incubated for 2 h at 37 °C with the epidermal side in contact with a solution of 0.5% trypsin in phosphate-buffered saline at pH 7.4. Trypsin is normally used to remove adherent cells from epidermis. After this time, the SC was washed with abundant Milli-Q water to remove the trypsin.[31,32]

Treatment of Skin Tissues with the Bicellar System. Two disks of whole skin with dimensions of approximately 2.5 cm^2 were used to carry out the experiment, which was performed in triplicate. The integrity of each sample was checked by determining the transepidermal water loss (TEWL) using a Tewameter TM210 (Courage-Khazaka, Köln, Germany) following the protocol described for absorption experiments.[30] One of the tissues was treated with water (control sample) and the other with the bicellar system (DOPC/DHPC). The treatment was realized placing the skin pieces SC side up, over a thin layer of water (but not submerged) on a Petri dish at 37 °C controlled by a thermostat. At these specific conditions samples were maintained completely hydrated. The treatment with bicellar system or with water consisted of four applications (every 1 h) of 13 μL of the bicellar system or water on the skin surface. After every application the samples were washed with Milli-Q water and left to dry before the following application. At the end of treatment (4 applications), every sample was washed with SLES solution (at 0.5% w/v) and later with Milli-Q water.

In addition, two more disks were used to determine the separated effect of the two structures forming the system. One of them was treated with the supernatant after centrifugation and the other with the precipitate. The treatment was the same as above-described, but the amount applied was higher with respect to the noncentrifuged system in order to increase the effect of each structure.

X-ray Scattering Measurements. *Small-Angle X-ray Scattering Measurements (SAXS).* SAXS measurements were performed at the European Synchrotron Radiation Facility (ESRF, Grenoble, France) using the Spanish beamline (BM16). The X-ray wavelength and the sample-to-detector distance were 0.9795 Å and 1422 mm, respectively. Scattering data were collected on a 2048 × 2048 pixel position-sensitive two-dimensional MAR CCD detector with an active surface area of 165 mm in diameter.[33] The tissue samples (control and treated with DOPC/DHPC system) were mounted into two sealed aluminum plates. Data conversion from 2D images to 1D curves (radial integration) were made using Fit2D software developed at the ESRF. The background was subtracted after normalization of all the curves with the counting rate of an ionization chamber.

Grazing Incidence Small-Angle X-ray Scattering Measurements (GISAXS). GISAXS measurements were carried out using a S3-MICRO (Hecus X-Ray Systems GmbH, Graz, Austria) coupled to a GENIX-Fox 3D X-ray source (Xenocs, Grenoble, France), which provided a detector-focused X-ray beam with a λ = 0.1542 nm Cu Kα line with more than 97% purity and less than 0.3% Kβ. The linear detector, PSD 50 Hecus, covered a range of 0.07 $nm^{-1} < q < 6$ nm^{-1}. Because of the use of a detector-focused small beam (300 × 400 μm fwhm) the scattering curves were mainly smeared by the detector width. This mainly produced a widening of the peaks without noticeable effect on the peak position for $q > 0.2$ nm^{-1}. Moreover, lamellae oriented parallel to the plane of incidence produce anisotropic scattering, which results in lower smeared scattering curves.

Hydrated samples were mounted by deposition on oxidized silicon (111) cut plane wafers. The wafers were oriented in the scanning direction by a stepping motor with a resolution of 0.01°. A homemade accessory allowed for the use of a humid atmosphere. Humid air at 22 °C was blown in the sample cell at 99% relative humidity. The sample−detector distance was fixed at 268 mm, and the exposure time was between 1800 and 3600 s. The sample was aligned between 0.5° and 0.25° of the incident angle.

The spatial calibration of the detectors in both dispositions was performed using silver behenate. In addition, both small-angle X-ray scattering measurements (transmission and grazing incidence) provide information about the larger structural units in the sample, namely, the repeat distance of a lamellar phase. The scattering intensity I (in arbitrary units) was measured as a function of the scattering vector q (in reciprocal nm). The latter is defined as

$$q = (4\pi \sin \theta)/\lambda$$

where θ is the scattering angle and λ the wavelength of the radiation (1.542 Å). The positions of the diffraction peaks are directly related to the repeat distance of the molecular structure, as described by Bragg's law:[34]

$$2d \sin \theta = n\lambda$$

in which n and d are the order of the diffraction peak and the repeat distance, respectively. In the case of a lamellar structure, the various peaks are located at equidistant positions; then

$$q_n = 2\pi n/d$$

q_n being the position of the nth order reflection.

Freeze-Substitution Transmission Electron Microscopy Experiments (FSTEM). The SC was cut into small ribbons with a size of approximately 2 × 1 mm. The ribbons were fixed in 5% (w/v) glutaraldehyde in 0.1 M sodium cacodylate buffer, pH 7.2, and postfixed in 0.2% (w/v) RuO_4 in sodium cacodylate buffer, pH 6.8 with 0.25% (w/v) potassium ferrocyanide ($K_4Fe(CN)_6$). After 1 h, the RuO_4 solution was replaced by fresh RuO_4 in order to establish an optimal fixation. After rinsing in buffer, the tissue samples were cryofixed, by rapid freezing on a liquid nitrogen cooled metal mirror (Cryovacublock, Leica) at −196 °C prior to freeze-substitution.

The freeze-substitution procedure was carried out in an AFS (automatic freeze substitution) system (Leica). The tissue samples were cryosubstituted at −90 °C for 48 h using 100% methanol, containing 1.0% (w/v) osmium tetroxide (OsO_4), 0.5% (w/v) uranyl acetate and 3.0% (w/v) glutaraldehyde. After the 48 h substitution period, the temperature was raised to −50 °C, the samples were washed 3 times in 100% methanol, and subsequently the methanol solution was gradually replaced by the embedding medium, Lowicryl HM20 (100%). This resin was replaced after 24 and 48 h by freshly made embedding medium. Finally the samples were transferred to a mold containing Lowicryl, and were incubated for 48 h at −50 °C under UVA radiation, to

allow polymerization. Ultrathin sections were cut (Ultracut UCT, Leica), transferred to Formvar-coated grids and examined in a Hitachi 600 transmission electron microscope.

Analysis of Micrographs by Cryo-TEM and FSTEM. For each sample, 10 overview and approximately 30−40 detail electron micrographs (for both techniques, cryo-TEM and FSTEM) were taken.[35] These micrographs were evaluated by five independent investigators, of which three were kept blind to the sample treatment. To quantify the data, a test circle of 3 cm in diameter was applied to suitable regions of pictures with identical magnifications, as described by Orci et al. in 1998.[35] By this method, the ratio of vesicle/tubular structures present in the system was quantified from the circles in the cryo-TEM micrographs. Additionally, the proportion of structures into and on skin was estimated from the circles in the FSTEM micrographs.

IR Experiments. Infrared spectra of the tissue samples were obtained using a 360-FTIR spectrophotometer Nicolet Avatar (Nicolet Instruments, Inc., Madison, WI) equipped with a 45° ZnSe thermal horizontal attenuated total reflection (ATR) crystal. All spectra were the average of 256 scans, collected within a period of 7 min at 2 cm^{-1} of resolution over the 4000−700 cm^{-1} region.

To collect the IR spectra, the skin sample was placed with the SC side down onto the ZnSe ATR crystal. In order to ensure reproducible contact between the sample and the crystal, we applied a pressure of 10 kPa on the samples. The spectra were collected at 32 °C (skin temperature), 37 °C (physiological temperature), and 45 °C (transition temperature of the SC lipids[36]). The temperature was controlled by a temperature controller integrated in the ATR device and by an external thermostatic jacket. The samples were placed in the equipment 30 min before collecting the spectra for temperature equilibration. Acquisition data were made with the support of OMNIC software.

RESULTS

Bicellar System Characterization. DLS and cryo-TEM techniques were used to characterize the bicellar system. The DLS technique provides more quantitative information about size of the system than the cryo-TEM technique. The size distribution curve analyzed by intensity of light scattered shows one peak centered on a population of particles with HD around 132 nm and a polydispersity index of 0.52 that is responsible for 100% of the light scattered. In order to confirm these results and to obtain morphological information about our sample, cryo-TEM was also used. Figure 1 shows two characteristic images of DOPC/DHPC bicellar system. Panels A and B display different views of the same sample. In panel A liposomes with diameters between 50 and 200 nm are observed. Panel B shows tubular structures with slightly smaller size than in panel A, i.e., sizes in the range of 30−120 nm. In spite of the fact that two kinds of structures are observed by cryo-TEM, only one peak is shown by DLS. This could be due to the wide difference in volume of both types of structures; the intensity of an individual vesicle of 100 nm in diameter with respect to a cylinder of 100 nm length and 3 nm diameter is approximately 300 times higher. Then, a higher contribution of the vesicles to the size calculated by DLS is expected. The relatively high polydispersity index can be explained by the presence of small and large vesicles.

These techniques are complementary in the sense that DLS offers better statistics, whereas cryo-TEM allows for the examination of detailed morphology of the structures. In addition, the analysis of cryo-TEM micrographs estimated an approximated ratio of vesicle/tubular structures in the system around 2.3 (70/30).

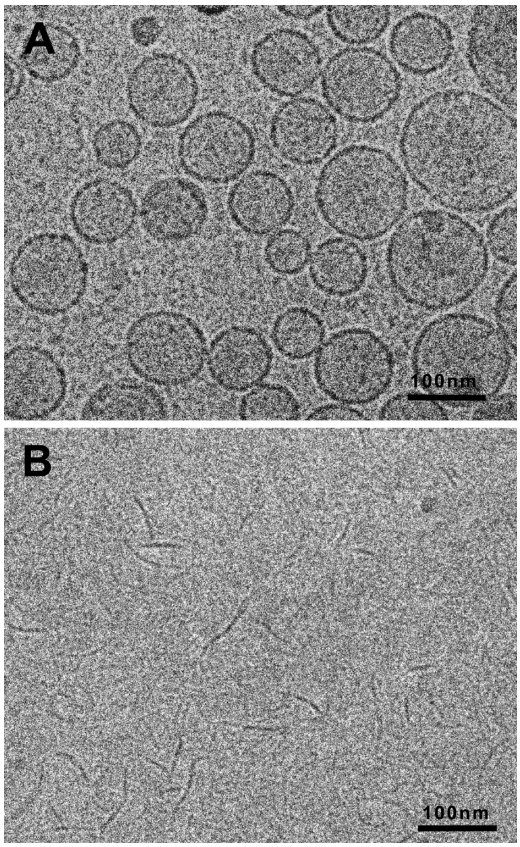

Figure 1. Representative micrographs of DOPC/DHPC bicellar system. Panels A and B display different views of the same sample. (A) Vesicle-shape structures and (B) tubular structures.

After centrifugation of the system, the supernatant and precipitate were measured by DLS. The supernatant size distribution curve analyzed by intensity shows two peaks centered on populations of particles with HD of 67.8 nm and 261 nm that are responsible for 6% and 32% of the light scattered, respectively. It is necessary to consider that, with this technique, particle size is approximated to that of a hypothetical hard sphere that diffuses with the same speed as the particle under examination. Since the supernatant would be formed principally by the light aggregates (tubular nonspherical structures visualized by microscopy), this measurement should be considered as an approximation. For the precipitate fraction, one peak centered on population of particle with HD of 394 nm (85.1%) is observed, that is compatible with the large vesicular structures observed by microscopy in the system.

Effect of DOPC/DHPC Bicellar System on the SC Lipids. The integrity of the skin membranes was checked for each sample by measuring the TEWL. The samples were stabilized for one hour in the bath, and TEWL was registered over one minute, after an initial 2 min stabilization of the probe on the skin. Following the Scientific Committee on Consumer Product (SCCP) opinion[37] and Organization for Economic Co-operation and Development Guideline,[38,39] TEWL values higher than 15 g m^{-2} h^{-1} are associated with disrupted membranes. In our experiments all TEWL values were less than 10 + 3 g m^{-2} h^{-1} that reflected the intactness of the pig skin.

dx.doi.org/10.1021/mp200075h | *Mol. Pharmaceutics* 2012, 9, 482−491

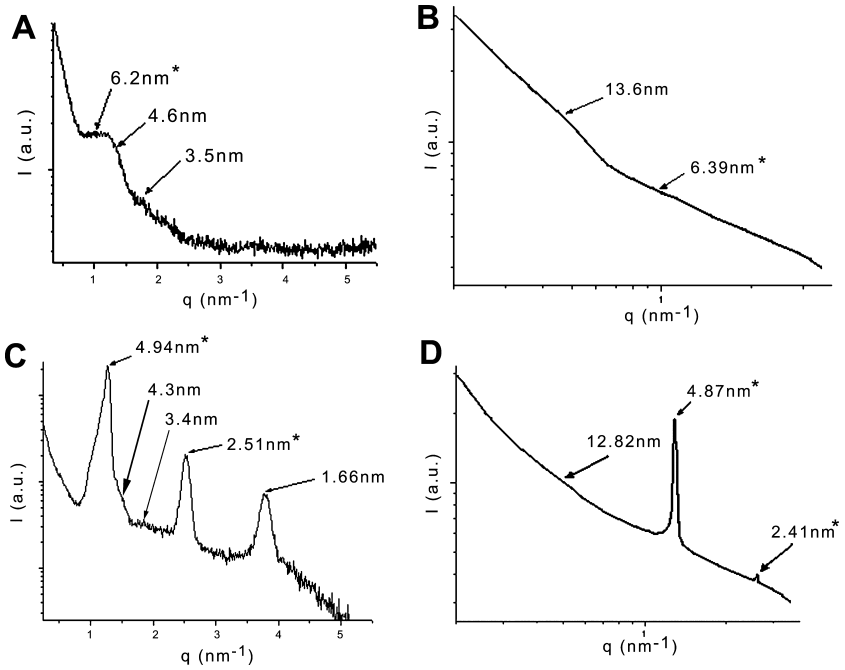

Figure 2. X-ray scattering profiles by GISAXS (left panels) and by SAXS (right panels). Panels A and B show the control sample, and panels C and D show the treated sample. The asterisk (*) shows the similar reflections by both dispositions.

X-ray Scattering. The X-ray scattering is a very useful technique to gather information about the larger structural units in the sample, for instance the repeat distances (*d*-spacing) of a lamellar phase,[18] which is related to the lamellar lipid structure in SC studies. Given the low amount of lipids in SC, to obtain a good signal, a very high quality and very sensitive instrumentation is necessary. Here, two different techniques that are based on X-ray scattering are compared for a better interpretation of the results. The grazing incidence small-angle X-ray scattering (GISAXS) technique has been used with a conventional source, and the skin surface was aligned with a certain incident angle; whereas the small-angle X-ray scattering (SAXS) technique has been used with a synchrotron source, and the skin surface is situated perpendicularly to the incident beam (transmission). Transmission SAXS requires a high-energy X-ray beam (synchrotron radiation) to obtain an acceptable scattering signal, since the X-rays interact only with a thin sample. Otherwise, GISAXS has an important advantage over the transmission method for films because the X-ray beam path length through the film plane is sufficiently long and a good intensity signal is obtained even using a conventional source.[40,41]

Figure 2 shows X-ray scattering profiles by GISAXS (left panels) and by SAXS (right panels). Panels A and B show the control sample and panels C and D the treated sample. The control sample from the GISAXS technique (panel A) shows a broad band that could be the overlap of two reflections, with scattering angle values (q) at 1.01 and 1.36 nm^{-1}, which are related to repeat distances around 6.2 and 4.6 nm, respectively. In addition, one reflection of lower intensity around 3.5 nm (q = 1.79 nm^{-1}) was observed. The control sample from the SAXS technique (panel B) shows two broad bands with scattering angle values (q) at 0.46 and 0.98 nm^{-1}, which are related to repeat distances around 13.6 and 6.39 nm, respectively. According to Jager et al.,[20] lipids of native SC are organized in two lamellar phases, one with a repeat distance around 13.5 nm, which corresponds to the large lamellar phase (LLP), and the other one with a repeat distance around 6 nm, which corresponds to the short lamellar phase (SLP). In our results, the SLP is observed by both techniques, reflection about 6 nm (see * in panels A and B). The first order of the reflection of LLP (~13 nm) is observed by SAXS, and GISAXS detected a reflection at 4.6 nm that could correspond to the third order of this LLP. The reflection of low intensity around 3.5 nm could correspond to the crystalline cholesterol[42] or to the fourth order of the LLP at d = 13.5 nm.

In the GISAXS pattern of the DOPC/DHPC treated sample (panel C) three sharp peaks (at q = 1.27, 2.50, and 3.78 nm^{-1}) that correspond to the distances at 4.94, 2.51, and 1.66 nm are clearly observed. Furthermore, one shoulder around 4.3 nm and a small band about 3.4 nm are noted, which are also found in the control sample (see panel A). The SAXS pattern of the treated sample (panel D) shows only two of these sharp peaks to the distances at 4.87 and 2.41 nm. Furthermore, the weak broad band around 13 nm is also observed after treatment such as is found in the control sample by the SAXS technique. Our results show that the treated sample exhibits strong peaks that correspond to diffraction orders (first, second and third, this last only observed by GISAXS) of a lamellar phase with a periodicity of about 5 nm (by both techniques, see * in panels C and D). This fact is compatible with a highly ordered lamellar structure in contrast with the weaker scattering bands detected in the control samples (panels A and B). This fact denotes the powerful interaction of the system with skin.

Freeze-Substitution Transmission Electron Microscopy. This technique allows one to fix the lipid lamellae and to examine individual lamellae in cross sections of the SC. In addition, the micrographs allow us to know the localization of the DOPC/DHPC system in the SC.

Figure 3 shows micrographs of native SC (left panels) and treated SC with DOPC/DHPC system (right panels). In this figure, corneocytes (C), flattened cells characterized by the absence of cell organelles and the presence of electron dense keratin filaments, and the lipid bilayers (L) within the intercellular spaces are clearly visualized. Panel A shows the surface

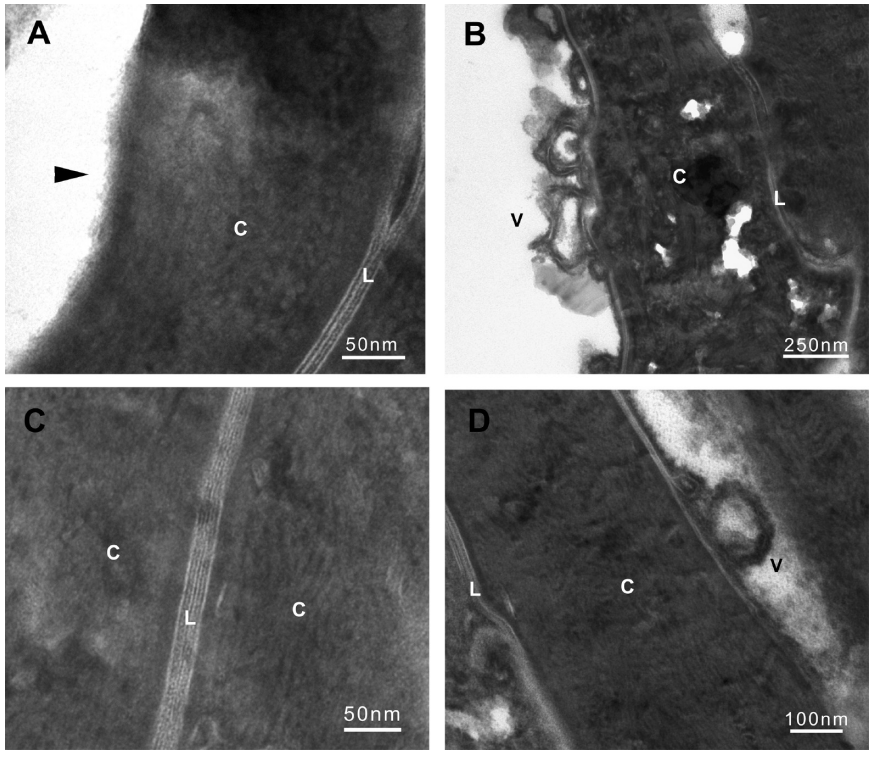

Figure 3. FSTEM micrograph of native SC (left panels) and treated SC with DOPC/DHPC system (right panels). Panels A and B are SC surface before and after treatment with the bicellar system, respectively. Panels C and D are enlargement of the lipid intercellular domains of SC before and after treatment with the bicellar system, respectively. Symbols: corneocytes (C), lipid bilayers (L), vesicle-like structures (V).

of the native SC (see black arrowhead). In addition, deeper down in the SC, lipid intercellular domains are observed. A more detailed overview of the lipid intercellular domains is shown in panel C. Here, the intact lipid bilayers exhibit the characteristic organization in an alternating pattern of electron-dense and lucent bands. In comparison with native SC, DOPC/DHPC treated SC shows presence of vesicle-like structures (V) adhered on the surface of the SC (see panel B). Furthermore, panel D is focused on lipid intercellular domains where the presence of vesicle-like structures (V) inside of this domain is clearly visualized. The analysis of the micrographs based on a modification of the test circle method described by Orci et al.[35] (see Experimental Section) indicated that, in samples treated with DOPC/DHPC, a minimum of 2% of the total circle area showed new vesicular structures into the skin. In native samples, new structures into the skin were not detected.

ATR-FTIR. ATR-FTIR spectroscopy is a technique in which the sample is placed directly onto an infrared transparent crystal. The penetration depth of IR in the skin is about 1 μm.[43] For this reason, this technique allows the investigation of the SC without isolation from the other skin layers. The effect of DOPC/DHPC nanostructures on the skin was evaluated by comparison of treated and untreated samples. Both samples were analyzed at different temperatures (32, 37, and 45 °C). The region analyzed was focused on the band associated with the alkyl chain of SC lipid vibration, CH_2 stretching mode (around 2900 and 2850 cm^{-1}). This region is particularly important because it provides information about the chain conformational order of the SC lipids.[44,45] There are two vibrations associated with the CH_2 stretching region: CH_2 symmetric and asymmetric vibrations (around 2850 and 2920 cm^{-1}, respectively). This study is focused on the CH_2 symmetric stretching vibration because it is more sensitive than the asymmetric vibration to packing changes.[46] Figure 4

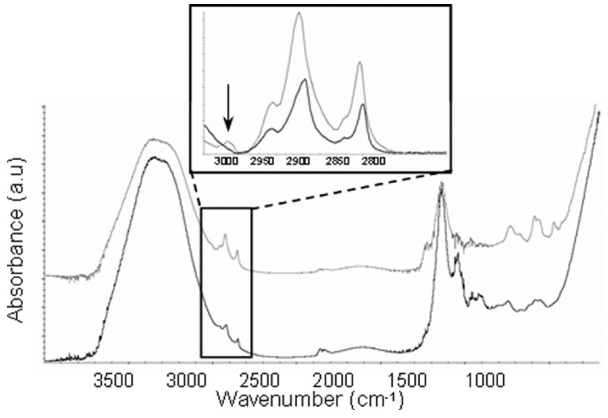

Figure 4. ATR-FTIR spectra of native SC (black line) and SC treated with the DOPC/DHPC system (gray line) at 32 °C. The inset shows the enlarged area from CH_2 symmetric stretching frequency for both samples, and the arrow shows the vibration of double bonds on DOPC.

shows the ATR-FTIR spectra of native SC and SC treated with DOPC/DHPC at 32 °C. In the inset, a shift in the CH_2 symmetric stretching frequency toward higher values is observed for treated sample. The arrow points to the characteristic vibration of double bonds on DOPC (CH=CH asymmetric stretching vibration, around 3007 cm^{-1}) for treated sample, indicating the presence of DOPC on the skin surface. Additionally, Table 1 shows the position of CH_2 symmetric vibration for skin samples before and after treatment with the

dx.doi.org/10.1021/mp200075h | *Mol. Pharmaceutics* 2012, 9, 482−491

Table 1. ATR-FTIR Values for the CH_2 Stretching Modes at Different Temperatures for Skin Samples before and after Treatment with the DOPC/DHPC Bicellar System

	CH_2 symmetric stretching (cm^{-1})	
temp (°C)	control	treated
32	2849.9 ± 0.21	2853.4 ± 0.19
37	2851.8 ± 0.6	2853.6 ± 0.27
45	2852.5 ± 0.28	2853.5 ± 0.20

DOPC/DHPC bicellar system at different temperatures. Before treatment with the DOPC/DHPC system (control sample), the increase of the temperature induces a shift of the CH_2 symmetric band to higher values, indicating an order−disorder transition from gel phase (2849.9 cm^{-1}, hexagonal organization) to the liquid-crystalline phase (2852.5 cm^{-1}); see Table 1. However, after treatment with the DOPC/DHPC bicellar system, the CH_2 stretching vibration did not show any change by increase of temperature, showing at all the temperatures studied a band around 2853 cm^{-1} compatible with a liquid-crystalline phase.

In order to determine the effect on skin of the different structures present in the system, two skin samples treated with the supernatant and the precipitate were analyzed by this technique. Figure 5 shows the ATR-FTIR spectra of SC treated

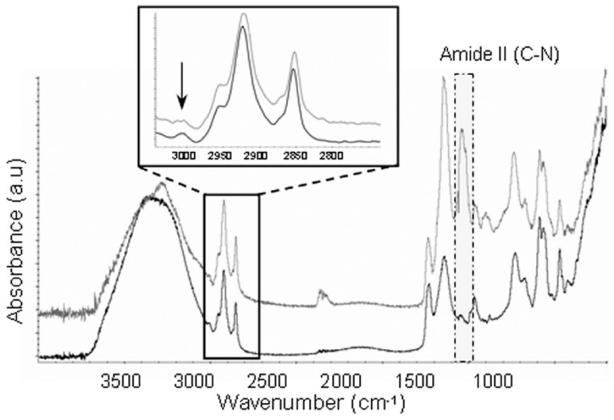

Figure 5. ATR-FTIR spectra of SC treated with the precipitate fraction (black line) and SC treated with the supernatant fraction (gray line) at 32 °C. The inset shows the enlarged area from the CH_2 symmetric stretching frequency for both samples; the arrow shows CH═CH asymmetric stretching vibration.

with precipitate (black line) and SC treated with supernatant (gray line) at 32 °C. Obviously, the signal in these spectra is more intense than those observed in Figure 4 due to the amount of sample applied being higher. In the inset, a light shift in the CH_2 symmetric stretching frequency is observed. The CH_2 frequency was 2854.07 cm^{-1} for sample treated with the precipitate and 2852.16 cm^{-1} for sample treated with supernatant. The CH═CH asymmetric stretching vibration from DOPC (see arrow) shows lower signal in sample treated with the supernatant (mainly tubular structures) than in sample treated with vesicle structures. In addition, a higher signal of the characteristic vibration of proteins, amide II (C−N vibration), is shown for sample treated with supernatant than for sample treated with the precipitate.

DISCUSSION

Bicellar Structure. The morphology of the bicellar systems is very versatile depending on several conditions, such as molar ratio between long-chain phospholipid and short-chain phospholipid, composition of the system and lipid concentration. Results from other bicellar systems formed from different long-chain phospholipids at different molar ratios indicated that the system with molar ratio 3.5 (chosen in this work), with a relatively low amount of DHPC, is appropriate for skin purposes.[16] It would be reasonable to think that a different molar ratio would induce a different effect, since the composition of this system is very important in its morphology and effect on the skin barrier function. Each phospholipid has a specific T_m depending on the length and saturation degree of the alkyl chain.[47] When this T_m is exceeded, the gel to liquid-crystalline phase transition occurs, and bicellar structures experience some morphological changes.[48] The more frequent long-chain phospholipids used to form these systems are DMPC or DPPC that have T_m of 23 and 41 °C, respectively. In this work another phospholipid of long-chain alkyl is used, DOPC, which has a very low T_m (−20 °C). Then, the experimental temperature is always higher than its T_m and different aggregates are expected. In fact, cryo-TEM showed tubular structures and vesicle-shaped structures. The formation of these structures would be due to the different distribution of the phospholipids in the different aggregates. DOPC is able to self-assemble forming lamellar phases, such as multilamellar vesicles,[49] and DHPC alone forms micelles in water. Given the hydrophilic character and the tendency of DHPC to favor regions with high curvature in lipid bilayers,[7] it is expected that the smaller structures (tubules) have a higher partition ratio of DHPC than the bigger structures (vesicles). In large vesicle-shaped structures the decreasing curvature becomes less attractive for DHPC being richer in DOPC. In addition, it is known that bilayers are able to incorporate a certain amount of surfactant molecules, but above this amount, the bilayer suffers from destabilization, fusion and even perforation; as a consequence the DHPC is finitely miscible with DOPC.[12] ATR-FTIR results of the skin treated separately with the two fractions of the system after centrifugation agree with the fact that vesicles are richer in DOPC than tubular structures. The sample treated with the precipitate (formed by vesicles) showed higher intensity in the characteristic vibration of double bonds CH═CH, only present in the DOPC molecule.

The composition of these vesicular structures could resemble the elastic vesicles, which are formed from phospholipid and surfactant.[50] Similar nanoaggregates have been described by several authors such as Nieh et al.,[51] Triba et al.[14] and Van Dam et al.,[52] who proposed a like hypothesis to describe different transitions undergone by the bicellar system. Different aggregates are formed as intermediates between two-dimensional networks of branched flattened cylindrical micelles and highly perforated lamellar sheets or vesicles. These aggregates could be the liposomes and tubular structures observed in this sample.

Effect on the SC Lipid Structure. After treatment with the DOPC/DHPC system, micrographs of FSTEM show that there are structures adhered to the SC surface whereas others are detected into the SC. This sample is composed of two structures with different morphology and possibly different composition. Our results demonstrate that these structures applied separately on the skin produce different effects on SC lipids. This indicates the strong influence of the self-assembly of lipid

nanostructures on their effect in the skin, a fact that has been previously reported.[7,53]

According to the results by ATR-FTIR technique, SC lipids are arranged in liquid-crystalline phase after treatment with the DOPC/DHPC system; the point of discussion is what event would induce this effect. Considering previous publications, the direct penetration of large vesicles into the narrow interlamellar spaces of SC appears to be difficult.[4,54] We assume that the vesicle-shaped structures are unable to penetrate because these structures are too large remaining adhered to the SC surface, as it is visualized by microscopy (Figure 3). This fact is supported by the results from SC treated with the precipitate rich in vesicles. The high intensity of the band associated to double band from DOPC beside the low intensity of the amide II band, would be related to a high accumulation of DOPC on the skin surface.

It could be expected that these structures adhered on the surface would serve as a superficial drug reservoir as previously have been reported by G. Cevc for colloid suspensions,[55] given that the incorporation of drug into this system is possible.[30] Additionally, the accumulation of DOPC (in liquid-crystalline phase) on the skin surface could cause in part the shift of the CH_2 vibrations to higher frequencies characteristic of a fluidification of lipids. However, the absence of any signal at 2849 cm^{-1} in the spectrum of treated sample (see Figure 2) indicates that also endogenous SC lipids after treatment are in a fluid state, since, if the bicellar system had not affected SC lipids, two peaks would have been observed on the CH_2 stretching region of treated sample: one from fluid DOPC (around 2853 cm^{-1}) and another at 2849 cm^{-1} (as in native sample) such as Boncheva et al.[19] reported. Another factor that could promote positively the fluidification of SC lipids is related to the penetration of free DOPC molecules into the SC as reported by Babu et al.[56] Other studies have shown similar spectral shifts in the CH_2 vibration of SC lipids by the effect of penetration of simple molecules.[57,58] Besides, penetration of other small structures, the tubular nanoaggregates containing DOPC, induce the same effect, such as is observed in SC treated with the supernatant fraction (rich in DOPC/DHPC tubular structures) (see Figure 5). This effect was described in a previous work by our group, in which the interaction of different bicellar systems with the skin was studied.[9,16]

The results by X-ray scattering (SAXS and GISAXS) also agree with these works since they evidence a high interaction of the system with skin. This interaction would be ruled by the part of the sample that penetrates into the skin, the free phospholipid molecules and the tubular structures. The SC treated with DOPC/DHPC had higher lamellar order than untreated SC (control sample), as evidenced by an increase in the intensity, sharpness and number of reflections associated with the short lamellar phase (SLP). Bouwstra et al. proposed a composition of this phase rich in cholesterol and in the linoleic moieties of ceramides 1 and 4.[59] Given that the SLP was altered after treatment with DOPC/DHPC, we assume a specific interaction of our systems with these sites. This fact was also observed previously after application of DPPC/DHPC bicelles[9] where the phospholipids from bicelles had also a tendency to be incorporated in the SC intercellular lipid, suggesting a reinforcement of the SLP of the SC. In that work DPPC/DHPC system lipids are incorporated as bilayers in the gel phase into the SC. In the present study, however, the DOPC/DHPC system is incorporated in the SC as bilayers in the liquid-crystalline phase inducing a fluidification of SC lipids as ATR-FTIR indicated. The effect is likely similar to oleic acid, which is incorporated into SC lipid bilayers forming microdomains in fluid phase.[60,61] It could be thought that the effect on the skin was caused by oleic acid from breakage or degradation of the covalent band C−O of DOPC. However, this possibility is ruled out at the experiment conditions used. Additionally this reasoning would involve that the effect on the skin promoted by DMPC/DHPC and DPPC/DHPC is the same as that promoted by myristic and palmitic acid respectively, and this is not the case. DMPC/DHPC bicelles exhibit an enhancer effect more superficial on skin,[9] and myristic acid penetrates deeper into the skin.[62] On the other hand, DPPC/DHPC bicelles are widely distributed at deeper layers of the skin[9] while palmitic acid is detected at superficial layers of the skin.[62]

The fact of some structures being incorporated into SC is supported by the micrographs of FSTEM (Figure 4). The structures visualized into SC (Figure 4D) would be a consequence of tubular structures, which could reconstitute to vesicles into SC by effect of the higher water content of SC, such as was previously reported for DPPC/DHPC bicelles. A part of the DHPC would partition to the medium, and DOPC would be mainly arranged in vesicles that remain immobilized inside the SC.[16] This transformation from small micelles and into vesicles was deeply studied for octyl glucoside (OG)/phosphatidylcholine (PC) micellar systems, and for these systems also the formation of new vesicular structures into the SC was observed.[4] In both cases a part of the molecules acting as mild surfactant (DHPC or OG) is removed from the micelles and the other part is included with the long-chain phospholipid bilayer to form vesicles in a similar way as in elastic vesicles.[50]

Summarizing, two different structures with two different interactions on SC lipid are found in the system studied. The bulkier structures can adhere to the surface of SC and can serve as a superficial drug reservoir. The small tubules could be the structures found in SC for their similar behavior to discoidal bicelles. Appropriate combination of both effects and the possibility to incorporate drugs would offer a range of possibilities for the DOPC/DHPC system in development of skin care products.

AUTHOR INFORMATION

Corresponding Author

*IQAC-CSIC, Department of Chemical and Surfactants Technology, C/ Jordi Girona 18-26, 08034 Barcelona, Spain. E-mail: gelen.rodriguez@cid.csic.es. Tel: 34-93 400 61 00. Fax 34-93 204 59 04.

Notes

The authors declare no competing financial interest.

ACKNOWLEDGMENTS

The authors wish to thank Elisenda Coll and Jaume Caelles for expert technical assistance, and also F. Fauth for his help in the BM16 (ESRF). M.C. is funded by the JAE-DOC program from CSIC (cofunded by FSE). This work was supported by funds from CICYT (CTQ 2010-16964) and from Generalitat de Catalunya (2009 SGR 1212). We are also indebted to Uni Gíslason for linguistic assistance.

ABBREVIATIONS USED

SC, stratum corneum; DOPC, 1,2-dioleyl-*sn*-glycero-3-phosphatidylcholine; DHPC, 1,2-dihexanoyl-*sn*-glycero-3-phosphatidylcholine; ATR-FTIR, attenuated total reflectance Fourier transform infrared spectroscopy; GISAXS, grazing incidence small-angle

X-ray scattering; SAXS, small-angle X-ray scattering; FSTEM, freeze-substitution transmission electron microscopy

REFERENCES

(1) Elias, P. M.; Feingold, K. R. Lipids and the epidermal water barrier: metabolism, regulation, and pathophysiology. *Semin. Dermatol.* **1992**, *11* (2), 176−182.

(2) López, O.; Cócera, M.; Wertz, P. W.; López-Iglesias, C.; de la Maza, A. New arrangement of proteins and lipids in the stratum corneum cornified envelope. *Biochim. Biophys. Acta* **2007**, *1768*, 521−529.

(3) Madison, K. C. Barrier function of the skin: "La raison d'être" of the epidermis. *J. Invest. Dermatol.* **2003**, *121*, 231−241.

(4) López, O.; Cócera, M.; López-Iglesias, C.; Walter, P.; Coderch, L.; Parra, J. L.; de la Maza, A. Reconstitution of liposomes inside the intercellular lipid domain of the stratum corneum. *Langmuir* **2002**, *18*, 7002−7008.

(5) Schaefer, H.; Redelmeier, T. E. *Skin barrier: Principles in percutaneous penetration*; Karger: Basel, Switzerland, 1996; pp 55−58.

(6) Wertz, P. W.; Downing, D. T. Ceramides of pig epidermis: structure determination. *J. Lipid Res.* **1983**, *24* (6), 759−765.

(7) Barbosa-Barros, L.; Barba, C.; Rodriguez, G.; Cocera, M.; Coderch, L.; Lopez-Iglesias, C.; de la Maza, A.; Lopez, O. Lipid nanostructures: self-assembly and effect on skin properties. *Mol. Pharmaceutics* **2009**, *6* (4), 1237−1245.

(8) Rodriguez, G.; Barbosa-Barros, L.; Rubio, L.; Cocera, M.; Diez, A.; Estelrich, J.; Pons, R.; Caelles, J.; De la Maza, A.; Lopez, O. Conformational changes in stratum corneum lipids by effect of bicellar systems. *Langmuir* **2009**, *25* (18), 10595−10603.

(9) Rodríguez, G.; Rubio, L.; Cócera, M.; Estelrich, J.; Pons, R.; De la Maza, A.; López, O. Application of Bicellar Systems on Skin: Diffusion and Molecular Organization Effects. *Langmuir* **2010**, *26* (13), 10578−10584.

(10) Vold, R. R.; Prosser, R. S. Magnetically oriented phospholipid bilayered micelles for structural studies of polypeptides. Does the ideal bicelle exist? *J. Magn. Reson. B* **1996**, *113*, 267−271.

(11) Dam, L. V.; Karlsson, G.; Edwards, K. Morphology of magnetically aligning DMPC/DHPC aggregates-perforated sheets, not disks. *Langmuir* **2006**, *28*, 3280−3285.

(12) Soong, R.; Macdonald, P. M. Water diffusion in bicelles and the mixed bicelle model. *Langmuir* **2009**, *25* (1), 380−390.

(13) Pabst, G.; Kucerka, N.; Nieh, M. P.; Rheinstadter, M. C.; Katsaras, J. Applications of neutron and X-ray scattering to the study of biologically relevant model membranes. *Chem. Phys. Lipids* **2010**, *163* (6), 460−479.

(14) Triba, M. N.; Devaux, P. F.; Warschawski, D. E. Effects of lipid chain length and unsaturation on bicelles stability. A phosphorus NMR study. *Biophysical J.* **2006**, *91* (4), 1357−1367.

(15) Barbosa-Barros, L.; Barba, C.; Cócera, M.; Coderch, L.; López-Iglesias, C.; de la Maza, A.; López, O. Effect of bicellar systems on skin properties. *Int. J. Pharm.* **2008**, *352*, 263−272.

(16) Barbosa-Barros, L.; de la Maza, A.; Estelrich, J.; Linares, A. M.; Feliz, M.; Walther, P.; Pons, R.; López, O. Penetration and growth of DPPC/DHPC bicelles inside the stratum corneum of the skin. *Langmuir* **2008**, *24*, 5700−5706.

(17) Yokomizo, Y.; Sagitani, H. The effects of phospholipids on the percutaneous penetration of indomethacin through the dorsal skin of guinea pig in vitro. 2. The effects of the hydrophobic group in phospholipids and a comparison with general enhancers. *J. Controlled Release* **1996**, *42*, 37−46.

(18) Pereira-Lachataignerais, J.; Pons, R.; Amenitsch, H.; Rappolt, M.; Sartori, B.; López, O. Effect of Sodium Dodecyl Sulfate at Different Hydration Conditions on Dioleoyl Phosphatidylcholine Bilayers Studied by Grazing Incidence X-ray Diffraction. *Langmuir* **2006**, *22* (12), 5256−5260.

(19) Boncheva, M.; Damien, F.; Normand., V. Molecular organization of the lipid matrix in intact stratum corneum using ATR-FTIR spectroscopy. *Biochim. Biophys. Acta* **2008**, *1778*, 1344−1355.

(20) de Jager, M. W.; Gooris, G. S.; Ponec, M.; Bouwstra, J. A. Lipid mixtures prepared with well-defined synthetic ceramides closely mimic the unique stratum corneum lipid phase behavior. *J. Lipid Res.* **2005**, *46*, 2649−2656.

(21) Winans, R. E.; Vajda, S.; Lee, B.; Riley, S. J.; Seifert, S.; Tikhonov, G. Y.; Tomczyk, N. A. Thermal Stability of Supported Platinum Clusters Studied by in Situ GISAXS. *J. Phys. Chem.* **2004**, *108* (47), 18105−18107.

(22) Babonneau, D.; Cabioc'h, T.; Naudon, A.; Girard, J. C.; Denanot, M. F. Silver nanoparticles encapsulated in carbon cages obtained by co-sputtering of the metal and graphite. *Surf. Sci.* **1998**, *409*, 358−371.

(23) Bouwstra, J. A.; Gooris, G. S.; van der Spek, J. A.; Bras, W. Structural investigations of human stratum corneum by small-angle X-ray scattering. *J. Invest. Dermatol.* **1991**, *97* (6), 1005−1012.

(24) Jadoula, A.; Doucetb, J.; Durandb, D.; Préat, V. Modifications induced on stratum corneum structure after in vitro iontophoresis: ATR-FTIR and X-ray scattering studies. *J. Controlled Release* **1996**, *42* (2), 165−173.

(25) Hallegot, P.; Minondo, A. M.; Fiat, F. Cryo-techniques applied to stratum corneum with description of a new sample holder for cryo-scanning electron microscopy of freeze-fractured samples. *J. Microsc.* **1999**, *196* (Part1), 35−39.

(26) Munford, M. L.; Lima, V. R.; Vieira, T. O.; Heinzelmann, G.; Creczynski-Pasa, T. B.; Pasa, A. A. AFM In-Situ Characterization of Supported Phospholipid Layers Formed by Vesicle Fusion. *Microsc. Microanal.* **2005**, No. Suppl. 3, 90−93.

(27) Honeywell-Nguyen, P. L.; Frederik, P. M.; Bomans, P. H.; Junginger, H. E.; Bouwstra, J. A. Transdermal delivery of pergolide from surfactant-based elastic and rigid vesicles: characterization and in vitro transport studies. *Pharm. Res.* **2002**, *19* (7), 991−997.

(28) Schmook, F. P.; Meingassner, J. G.; Billich, A. Comparison of human skin or epidermis models with human and animal skin in in-vitro percutaneous absorption. *Int. J. Pharm.* **2001**, *215* (1−2), 51−56.

(29) Tan, G.; Xu, P.; Lawson, L. B.; He, J.; Freytag, L. C.; Clements, J. D.; John, V. T. Hydration Effects on Skin Microstructure as Probed by High- Resolution Cryo-Scanning Electron Microscopy and Mechanistic Implications to Enhanced Transcutaneous Delivery of Biomacromolecules. *J. Pharm. Sci.* **2010**, *99* (2), 730−740.

(30) Rubio, L.; Alonso, C.; Rodriguez, G.; Barbosa-Barros, L.; Coderch, L.; De la Maza, A.; Parra, J. L.; Lopez, O. Bicellar systems for in vitro percutaneous absorption of diclofenac. *Int. J. Pharm.* **2010**, *386* (1−2), 108−113.

(31) López, O.; De la Maza, A.; Coderch, L.; Parra, J. L. Formation and Characterization of Liposomes from Lipid/Proteic Material Extracted from Pig Stratum Corneum. *J. Am. Oil Chem. Soc.* **1996**, *73*, 443−448.

(32) Norlen, L.; Emilson, A.; Forslind, B. Stratum corneum swelling. Biophysical and computer assisted quantitative assessments. *Arch. Dermatol. Res.* **1997**, *289* (9), 506−513.

(33) Rueda, D. R.; García-Gutiérrez, M. C.; Nogales, A.; Capitán, M. J.; Ezquerra, T. A.; Labrador, A.; Fraga, E.; Beltrán, D.; Juanhuix, J.; Herranz, J. F.; Bordas, J. Versatile wide angle diffraction setup for simultaneous wide and small angle x-ray scattering measurements with synchrotron radiation. *Rev. Sci. Instrum.* **2006**, *77* (3), 033904-1−033904-5.

(34) Bragg, W. L. The diffaction of short electromagnetic waves by a crystal. *Proc. Cambridge Philos. Soc.* **1913**, *17*, 43−57.

(35) Orci, L.; Perrelet, A.; Rothman, J. E. Vesicles on strings: morphological evidence for processive transport within the Golgi stack. *Proc. Natl. Acad. Sci. U.S.A.* **1998**, *95* (5), 2279−2283.

(36) Plasencia, I.; Norlén, L.; Bagatolli, L. A. Direct visualization of lipid domains in human skin stratum corneum̀s lipid membranes: effect of pH and temperature. *Biophys. J.* **2007**, *93*, 3142−3155.

(37) SCCP. *Opinion on ethyl lauroyl arginate HCl*; 2008, 1−60.

(38) OECD. *Guidance document for the conduct of skin absorption studies*; OECD Series on Testing and Assessment: Number 28; 2004.

(39) Frelichowska, J.; Bolzinger, M. A.; Pelletier, J.; Valour, J. P.; Chevalier, Y. Topical delivery of lipophilic drugs from o/w Pickering emulsions. *Int. J. Pharm.* **2009**, *371* (1−2), 56−63.
(40) Byeongdu, L.; Jinhwan, Y.; Weontae, O.; Yongtaek, H.; Kyuyoung, H.; JIN, K. S.; Jehan, K.; Kwang-Woo, K.; Moonhor, R. In-situ grazing incidence small-angle X-ray scattering studies on nanopore evolution in low-k organosilicate dielectric thin films. *Macromolecules* **2005**, *38* (8), 3395−3405.
(41) Hsua, C.-H.; Jenga, U.-S.; Leea, H.-Y.; Huanga, C.-M.; Lianga, K. S.; Windoverb, D.; Lub, T.-M.; Jinc, C. Structural study of a low dielectric thin film using X-ray reflectivity and grazing incidence small angle X-ray scattering. *Thin Solid Films* **2005**, *472* (1−2), 323−327.
(42) Caussin, J.; Gooris, Gert S.; Janssens, Michelle; Joke, A. Bouwstra. Lipid organization in human and porcine stratum corneum differs widely, while lipid mixtures with porcine ceramides model human stratum corneum lipid organization very closely. *Biochim. Biophys. Acta* **2008**, *1778*, 1472−1482.
(43) Coderch, L.; Pera, M. d.; Perez-Cullell, N.; Estelrich, J.; Maza, A. d. l.; Parra, J. L. The effect of liposomes on skin barrier structure. *Skin Pharmacol. Appl. Skin Physiol.* **1999**, *12*, 235−246.
(44) Gooris, G. S.; Bouwstra, J. A. Infrared spectroscopic study of stratum corneum model membranes prepared from human ceramides, cholesterol, and fatty acids. *Biophys. J.* **2007**, *92*, 2785−2795.
(45) Prasch, T.; Knübel, G.; Schmidt-Fonk, K.; Ortanderl, S.; Nieveler, S.; Förster, T. Infrared spectroscopy of the skin: influencing the stratum corneum with cosmetic product. *Int. J. Cosmet. Sci.* **2000**, *22*, 371−383.
(46) Mendelsohn, R.; Flach, C. R.; Moore, D. J. Determination of molecular conformation and permeation in skin via IR spectroscopy, microscopy, and imaging. *Biochim. Biophys. Acta* **2006**, *1758*, 923−933.
(47) Williams, W. P.; Cunningham, B. A.; Wolfe, D. H.; Derbyshire, G. E.; Mant, G. R.; Bras, W. A combined SAXS/WAXS investigation of the phase behaviour of di-polyenoic membrane lipids. *Biochim. Biophys. Acta* **1996**, *1284* (1), 86−96.
(48) Diller, A.; Loudet, C.; Aussenac, F.; Raffard, G.; Fournier, S.; Laguerre, M.; Grelard, A.; Opella, S. J.; Marassi, F. M.; Dufourc, E. J. Bicelles: A natural 'molecular goniometer' for structural, dynamical and topological studies of molecules in membranes. *Biochimie* **2009**, *91* (6), 744−751.
(49) Nilsson, A.; Holmgren, A.; Lindblom, G. Fourier-transform infrared spectroscopy study of dioleoylphosphatidylcholine and monooleoylglycerol in lamellar and cubic liquid crystals. *Biochemistry* **1991**, *30* (8), 2126−2133.
(50) Choi, M. J.; Maibach, H. I. Elastic vesicles as topical/transdermal drug delivery systems. *Int. J. Cosmet. Sci* **2005**, *27*, 211−221.
(51) Nieh, M. P.; Raghunathan, V. A.; Glinka, C. J.; Harroun, T. A.; Pabst, G.; Katsaras, J. Magnetically alignable phase of phospholipid "bicelle" mixtures is a chiral nematic made up of wormlike micelles. *Langmuir* **2004**, *20* (19), 7893−7897.
(52) van Dam, L.; Karlsson, G.; Edwards, K. Direct observation and characterization of DMPC/DHPC aggregates under conditions relevant for biological solution NMR. *Biochim. Biophys. Acta* **2004**, *1664* (2), 241−256.
(53) Foldvari, M.; Badea, I.; Wettig, S.; Baboolal, D.; Kumar, P.; Creagh, A. L.; Haynes, C. A. Topical delivery of interferon alpha by biphasic vesicles: evidence for a novel nanopathway across the stratum corneum. *Mol. Pharmaceutics* **2010**, *7* (3), 751−762.
(54) Knepp, V. M.; Szoka, F. C. J.; Guy, R. H. Controlled drug release from a novel liposomal delivery system. II. Transdermal delivery characteristics. *J. Controlled Release* **1990**, *12*, 25−30.
(55) Cevc, G. Lipid vesicles and other colloids as drug carriers on the skin. *Adv. Drug Delivery Rev.* **2004**, *56* (5), 675−711.
(56) Babu, S.; Fan, C.; Stepanskiy, L.; Uitto, J.; Papazoglou, E. Effect of size at the nanoscale and bilayer rigidity on skin diffusion of liposomes. *J. Biomed. Mater. Res.* **2009**, *91A*, 140−148.
(57) Guillard, E. C.; Tfayli, A.; Laugel, C.; Baillet-Guffroy, A. Molecular interactions of penetration enhancers within ceramides organization: A FTIR approach. *Eur. J. Pharm. Sci.* **2009**, *3 6*, 192−199.
(58) Harrison, J. E.; Groundwater, P. W.; Brain, K. R.; Hadgraft, J. Azone® induced fluidity in human stratum corneum. A fourier transform infrared spectroscopy investigation using the perdeuterated analogue. *J. Controlled Release* **1996**, *41*, 283−290.
(59) Bouwstra, J. A.; Dubbelaar, F. E.; Gooris, G. S.; Ponec., M. The lipid organisation in the skin barrier. *Acta Derm.-Venereol., Suppl.* **2000**, *208*, 23−30.
(60) Ongpipattanakul, B.; Burnette, R. R.; Potts, R. O.; Francoeur, M. L. Evidence that oleic acid exists in a separate phase within stratum corneum lipids. *Pharm. Res.* **1991**, *8*, 350−354.
(61) Hathout, R. M.; Mansour, S.; Mortada, N. D.; Geneidi, A. S.; Guy, R. H. Uptake of microemulsion components into the stratum corneum and their molecular effects on skin barrier function. *Mol. Pharmaceutics* **2010**, *7* (4), 1266−1273.
(62) Cotte, M.; Dumas, P.; Besnard, M.; Tchoreloff, P.; Walter, P. Synchrotron FT-IR microscopic study of chemical enhancers in transdermal drug delivery: example of fatty acids. *J. Controlled Release* **2004**, *97*, 269−281.